



HAL
open science

A Modular SHM-Scheme for Engineering Structures under Changing Conditions: Application to an Offshore Wind Turbine

Moritz Häckell, Raimund Rolfes

► **To cite this version:**

Moritz Häckell, Raimund Rolfes. A Modular SHM-Scheme for Engineering Structures under Changing Conditions: Application to an Offshore Wind Turbine. EWSHM - 7th European Workshop on Structural Health Monitoring, IFFSTTAR, Inria, Université de Nantes, Jul 2014, Nantes, France. hal-01020451

HAL Id: hal-01020451

<https://inria.hal.science/hal-01020451>

Submitted on 8 Jul 2014

HAL is a multi-disciplinary open access archive for the deposit and dissemination of scientific research documents, whether they are published or not. The documents may come from teaching and research institutions in France or abroad, or from public or private research centers.

L'archive ouverte pluridisciplinaire **HAL**, est destinée au dépôt et à la diffusion de documents scientifiques de niveau recherche, publiés ou non, émanant des établissements d'enseignement et de recherche français ou étrangers, des laboratoires publics ou privés.

A MODULAR SHM-SCHEME FOR ENGINEERING STRUCTURES UNDER CHANGING CONDITIONS: APPLICATION TO AN OFFSHORE WIND TURBINE

Moritz W. Häckell¹, Raimund Rolfes¹

¹ *Institute of Structural Analysis, Leibniz Universität Hannover, Appelstraße 9A, 30169 Hannover*

m.haekell@isd.uni-hannover.de, r.rolfes@isd.uni-hannover.de

ABSTRACT

Many countries worldwide and in Europe still have the goal of a future cut of CO₂ emission in common. A shift from fossil to renewable energy source is the logical consequence. (Offshore) wind turbines ((O)WTs) play an important role in the so called "green" energy sector. An increasing number of remote offshore plants and an ageing fleet of onshore structures raise the demand of structural health monitoring (SHM) in this field. Guidelines still lack firm establishments and SHM is supposed to help assuring a safe operation and a possible extension of the lifetime.

The work presented displays a modular SHM scheme applicable for engineering structures under varying environmental and operational conditions (EOCs). The procedure is applied to a 5MW OWT in the German bight, located in the test field *alpha ventus*. The integration into and application of the complete SHM scheme is presented through different condition parameters (CPs), machine learning (data classification) and hypothesis testing.

KEYWORDS : *Offshore Wind Turbine, Machine Learning, Condition Parameter, Control Charts, Affinity Propagation*

INTRODUCTION

It is widely accepted that monitoring of large scale (civil engineering) structures' necessitates accounting for the structures' current state. In general, variations in the structures response are caused by variations in the environmental and operational conditions (EOCs). For (O)WT or bridges, these can be of diverse kinds as temperature (gradients), wind speed, turbulence intensity, traffic volume and type and wave period and heights. All these influences may change the characteristics of the dynamic response and hence potentially the monitored condition parameter(s).

To achieve the task of monitoring a complex, large scale engineering structure, SHM faces different difficulties. Not only two different states of the structure must be compared but all important EOCs must be taken into account to represent all healthy conditions. Hence, for OWTs a learning phase is required to cover the differing behavior over yearly seasons. Next, type, location and extend of damage can vary strongly which leads to the intention that a single damage parameter might not be sufficient for a good SHM performance. Last but not least, to be of use for owners and operators, the monitored parameters must be put into a probabilistic context and an intelligible layout. All of these steps are targeted here for the OWT.

In many cases, SHM is divided into four general, subsequent steps after Rytter [1]: Damage -detection, -localization, -quantification, and -prediction. While this is a general description of SHM-goals, their implementation remains open. To achieve the purposes of SHM, many different techniques are available and clarification needs to be given on what purpose they are used for. Figure 1 shows the modular SHM-scheme applied. Four general (structure-independent) steps are displayed, which give the tools to approach the (first two) SHM goals. Monitoring is divided into training and testing phase (dashed lines). Within the later one, a decision about the current system state is possible:

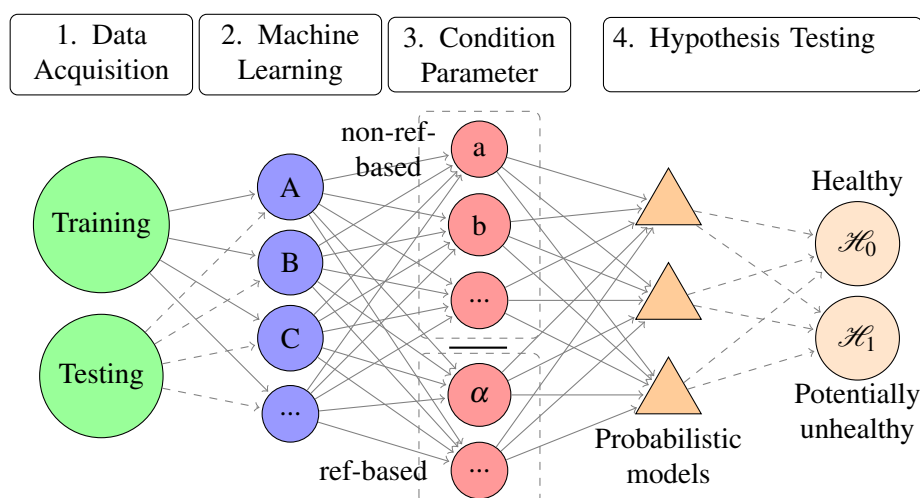


Figure 1 : Modular SHM-scheme: Training and subsequently testing data sets are analyzed through a combination of machine learning algorithm, damage parameter and probabilistic model to draw a decision.

- Training phase
 - **Data acquisition**, initial data base comprised of valid and sound data sets;
 - **Machine learning** (ML), to combine/train data of differing system states¹;
 - Estimation of **condition parameter**(s) (CPs);
 - Development of **probabilistic models** for CPs with respect to ML;
- Testing phase
 - **Data acquisition** of new, incoming data sets (usually 10 min. blocks for OWTs);
 - **Machine learning** for data set assignment;
 - Calculation of **CP**(s) (if necessary, with respect to machine learning);
 - **Hypothesis testing** (HT) through evaluation of CP(s) within probabilistic model(s);

The following chapter will introduce the analyzed OWT structure including data acquisition and the recorded data base, followed by a chapter giving an overview of possible and implemented techniques to realize the proposed SHM steps. The article proceeds with the presentation of a subset of results from the full size plant and closes with a conclusion section.

1. THE OFFSHORE WIND TURBINE

For scientific and commercial purposes a 5MW AREVA M5000–116 OWT was equipped with several hundred sensors. The plant is located in the test field *alpha ventus* within the German Bight, erected in a water depth of about 30 m in 2009. Here, data sets from March 1st 2010 till April 12th 2011 were analyzed. Figure 2 shows the investigated sensor locations and structural dimensions (1,500,000 kg total mass). A summary of structural dynamics and extracted modal properties can be found in [2] and [3]. Each data set consists of time series from 24 accelerometers over a period T of ten minutes, with a sampling rate f_s of 50 Hz. For further investigations, 13 EOCs² were chosen to build the data base along with the system's dynamic response. Accordingly, each data sets consists of 10 min mean values for the EOCs and 50 Hz acceleration signals. After a plausibility check, 19,135 of initially 33,343 data sets remain in the data base for further analysis. To underline the need for machine

¹This step is often also referred to as data normalization and might be applied subsequently to the estimation of condition parameters, depending on the procedure chosen.

²1. Rotor speed in RPM, 2. Wind speed in m/s, 3. Nacelle position (rel) in deg, 4. Temperature in °C, 5. Turbulence intensity, 6. Wave H_s in m, 7. Wave mean Period in s, 8. Rel wind direction in deg, 9. Pressure in hPa (mbar), 10. Wave direction in deg, 11. Temp difference 40-100 m in °C, 12. Wind direction in deg, 13. Generator speed in RPM

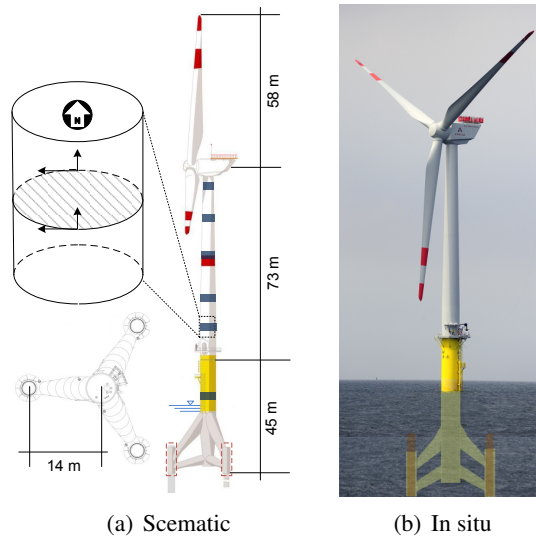


Figure 2 : 2(a) Tripod structure with acceleration sensor locations (blue rectangles), measurement directions for each level (upper left) and footprint of tripod (lower left) and 2(b) OWT in operation [2].

learning and hence accounting for EOC-variations in later SHM steps, Figure 3 shows power spectral densities (PSD) $S_{xx}(\omega)$ (3(a)) and accumulated energy (AE) levels $E_{xx}(\omega)$ (3(b)) for different system states using wind speed as a major system variable. Since wind speed drives excitation levels, rotor speed and in higher regimes the pitch angle, differing frequency contents and energy distributions appear. It is obvious, that many condition parameters will be influenced by this change in dynamic behavior. Here, $S_{xx}(\omega)$ is the Fourier transform of the auto-correlated time signal $\Phi_{xx}(\tau)$ for a single sensor x as

$$S_{xx}(\omega) = F\{\Phi_{xx}(\tau)\} \quad (1)$$

and $E_{xx}(\omega)$ as normalized sum of $S_{xx}(\omega)$, with

$$\hat{E}_{xx}(\omega_i) = \sum_{n=1}^i S_{xx}(\omega_n) \quad (2)$$

$$E_{xx}(\omega_i) = \frac{100 * \hat{E}_{xx}(\omega_i)}{\hat{E}_{xx}(\omega_i = \frac{f_s}{2})}. \quad (3)$$

The AE is an indicator for energy distribution within a signal, taking changes in the whole frequency range into account instead of tracking single peaks. It was used for instance for shape analysis [4] and to characterize earthquakes in time domain [5]. The mean frequency between 90 and 100% AE-levels for single sensors, is used as a CP later on.

2. SHM FOR LARGE SCALE STRUCTURES

Originating from a plausible data base, it is important to clearly distinguish between machine learning procedures and CPs. Even though these two come closely linked in most cases and a combination of both will always be necessary, their task is different. The CP is the monitored value while machine learning captures a dependency between CP and system states. The close relationship sometimes leads to confusion. As an illustrating example, Fritzen et al. [6] use CPs from stochastic subspace identification (SSI) in a sophisticated SHM scheme as goal values not as machine learning technique. Machine learning is done through a multi dimensional fuzzy classification of temperature measurements.

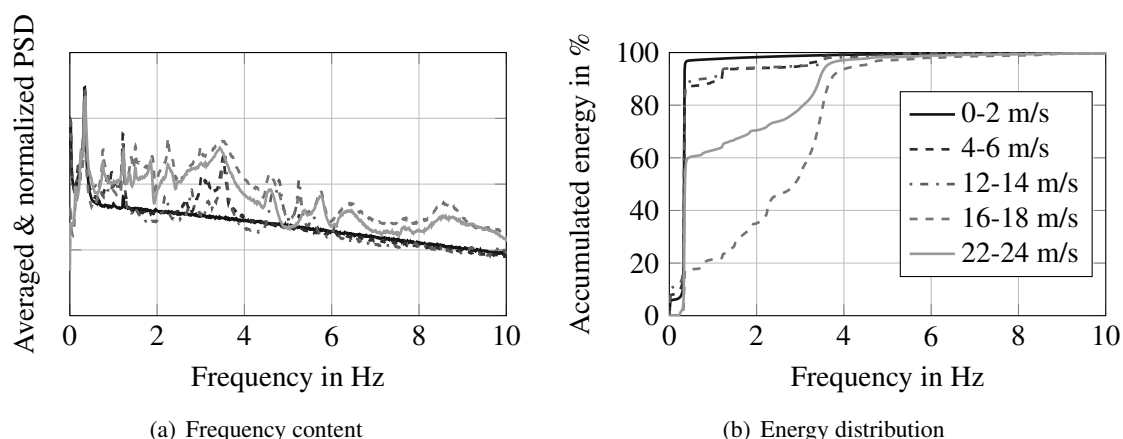


Figure 3 : Dynamic characteristics for AREVA M5000 wind energy converter for different wind speeds (100 randomly chosen data sets per wind class, sensor 71.2 m above sea bed).

In general, two fundamentally different approaches to machine learning in SHM for operating structures are present in the literature: On the one hand, the task of taking changes in dynamic responses into account is targeted without the actual measurement of EOCs, on the other hand, given EOC information is used to track changes and feed normalization procedures. The former is obviously independent from EOC measures and avoids the procedure of choosing and (potentially additionally) measuring these values. By omitting EOCs, this class must solely rely on extracted features from response signals and often limits the CP choice. Further more, these attempts potentially ignore damaged conditions that appear similar to healthy conditions in another learned state. The latter approach takes advantage of additional information but also implies that the chosen EOCs are sufficient to describe all important system states. In the case of OWTs, several EOCs feed in or are targeted by the control of the plant and therefore are part of the turbine's initial set-up.

Machine learning is usually split into supervised (regression) and unsupervised (clustering) approaches. In SHM, neural networks have been applied e.g. by Sohn [7, 8], principal component analysis [9] and clustering [10] are also popular techniques.

For the presented study a new clustering technique dubbed affinity propagation (AP) is used. The algorithm was developed by Frey and Duek [11, 12] and introduced to the field of SHM in [3]. AP evolves the number of resulting clusters automatically based on a given, negative valued 'preference' for each data point and an iterative process of "messages-passing" between data points [11]. The 'preference' can be understood as a kind of gravity that makes a certain point preferable as cluster center. AP_n indicates an AP run with preference n for all data points.

After machine learning, one has to decide for CPs (features) to be monitored. In the authors opinion it is important to separate between reference- and non-reference-based CP: The first type of parameter is a comparison between two states by definition and necessitates (at least) two data sets for its estimation. Hence, it is dependent on the machine learning type and set-up. The second type can be calculated from a single data set only with a subsequent comparison to other data sets.

Standard (non-ref-based) statistical CPs can be taken directly from the recorded time series as there are mean, maximum, standard deviation, skewness and kurtosis. The significant acceleration (or velocity/strain etc.) is calculated as the mean of the highest third of values and borrowed from ocean statistics where the significant wave height is used regularly. Modal parameters are used very frequently to trace the structures state, often linked to temperature changes [9, 13, 14]. With modal parameters, the problem of their automated extraction comes into place since their calculation is not straightforward. To estimate modal parameters for the OWT, the triangulation-based extraction of modal parameters (TEMP) is used here [2, 3, 15]. Frequencies correlated with accumulated energy-

levels as described in Equation (2) and (3) form new parameters. Complete frequency spectra can also be taken as multidimensional parameters [16, 17]. Reference-based residues from stochastic subspace identification (SSI) [3, 6, 18] or vector autoregressive models (VAR) [3, 19] have also become popular CPs. A selection of these parameters is applied here.

A further important tool for hypothesis testing are so-called control charts where a control variable is plotted over time [20]. Upper- and lower control limit (UCL/LCL) indicate value regions for 'normal' behavior, the healthy state or \mathcal{H}_0 -hypothesis in the present case. Kullaa uses different control charts for SHM at a wooden bridge model and a vehicle crane [21]. Here, a standardized residual control chart with varying LCL/UCL is introduced. In the previous steps, every incoming data set was assigned to a cluster where a parameter distribution is present for each CP-type. These distributions are not necessarily of known kind and might be non-symmetric. LCL and UCL are defined as 0.1 and 99.9% percentiles, respectively. Which leads to the following definition of the control variable $z_{i,j}^X$ as

$$z_{i,j}^X = \begin{cases} \frac{\overline{CP}_{i,j}^X}{|CP_{50}^{X,j,c_k} - CP_{99.9}^{X,j,c_k}|} & \text{for } \overline{CP}_{i,j}^X > 0 \\ \frac{\overline{CP}_{i,j}^X}{|CP_{50}^{X,j,c_k} - CP_{0.1}^{X,j,c_k}|} & \text{for } \overline{CP}_{i,j}^X < 0 \end{cases} \quad \text{with } \overline{CP}_{i,j}^X = CP_{i,j}^X - CP_{50}^{X,i,j}. \quad (4)$$

Where CP_n^{X,j,c_k} is the n% percentile for CP X in classification j and cluster c_k and $CP_{i,j}^X$ is the CP X estimated for the i-th incoming data set (with respect to classification j), see also Figure 4 and 5. **It should be emphasized, that, according to the suggested SHM structure, every SHM-procedures consists of, and hence can be categorized in, three constituents (even if included passively or unintentionally): Machine Learning – Condition Parameter – Hypothesis Testing.**

3. MONITORING THE OWT

The following chapter outlines the application of the introduced SHM scheme to the OWT. It is obvious from Figure 1 that the number of resulting decisions in HT (e.g. through control charts) rapidly increases with machine learning types and CPs. Hence, major steps will be displayed through a specific set-up for classification (as ML) in combination with two CPs, namely VAR-residues. Finally, different CPs and classification types are compared by means of false-positive alarms within the control charts. As stated in Section 1., the initial data set is formed from 19,135 sets with 13 EOCs available for each set. In the first step, AP is chosen as machine learning algorithm and the data base is split into a training- (set 1 to 17,119) and testing-phase (set 17,120 to 19,135).

3.1 Training phase

A subset of 2016 randomly chosen sets (2 weeks) is taken from the learning-phase to train the system. One manual classification by wind speed and four AP set-ups, named 'AP1' to 'AP4', are executed (see Table 1). The AP uses EOCs normalized to a range of [-1;0] each. All set-ups differ in number and type of selected EOCs and resulting number of clusters. For classification 'AP2' Figure 4(a) shows the EOC distributions for each of the seven resulting clusters. Distributions for each cluster per EOC are combined. AP groups the data sets in this five-dimensional EOC-space very well and each cluster spans different EOC ranges. Each data set is assigned to a single cluster and hence reference-based CPs can also be calculated.

Since the VAR-residue (CP^{R^2}) is a reference-based CP, each data set in a cluster is compared to a mean reference matrix of the cluster, VAR-parameters in this case. The results can be seen in Figure 4(b) where $-(CP^{R^2} - 1)$ is plotted in logarithmic scale³ and grouped per cluster (1-7).

³ $CP^{R^2} \in [-\infty, 1]$; A value of 1 corresponds to good agreement between reference and current data set. The transformation is done to allow logarithmic scaling. Accordingly, large values indicate bad agreement between reference and actual data set.

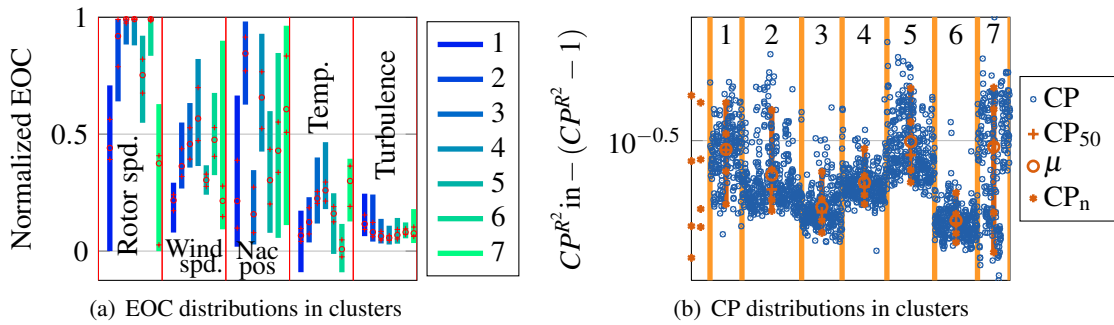


Figure 4 : 4(a) EOC distributions for cluster 1 to 7 in classification "AP2". Here, 5/95%, 25/75% and median are marked by bars, "+" and "o", respectively. 4(b) Corresponding distribution of VAR-residue sorted by clusters. CP given with mean (μ), median (CP_{50}), and percentiles ($CP_n, n = 5, 25, 75, 95$). Distributions for non-clustered data in very left section.

Clearly, the CP^{R^2} has a distinctively different distribution for the different clusters. The distributions for non-clustered data are indicated in the very left section: The very left marks indicate a distribution where each data set is compared to its predecessor, with good results but the draw-back of omitting consecutive degradation. The right marks in the very left section result from single training cluster.

All other CP are processed accordingly, resulting in CP distributions for each cluster in each classification. Note, that non-reference-based CPs are calculated only once, while reference based CPs need to be re-calculated for each classification set-up since data set assignment to clusters and hence the reference matrices change. The CP-distributions per cluster can now be used to evaluate new incoming data sets for the testing phase.

3.2 Testing phase

For testing, 2016 successive data sets were chosen from the testing-part of the data base and processed. For validity, the distribution of EOC values during testing was checked against the training phase: Distribution densities differ, but all testing EOC-ranges are covered in the training phase. The testing phase can be carried out for each classification type. In a first step, a new data set is assigned to a cluster by minimum normalized EOCs-distances. Afterwards, the CP is calculated and compared to the CP-distribution learned for the specific cluster (and classification). To draw a control chart as described in 2., the CP is compared to median and 0.1 or 99.9%-percentile (see equation (4)) to range between [-1,1] for acceptance of the \mathcal{H}_0 -hypothesis.

Figure 5 displays such a normalized control chart for CP^{R^2} and CP^{MBox} in 'AP2' with lower and upper control limits. The control variable is plotted chronologically for all 2016 data sets and out-of-control points (\mathcal{H}_1 -hypothesis) can be detected in 3.22%/0.69% of the data sets. Considering the limited training period, slightly differing EOCs and the fast return of CP^{R^2} and CP^{MBox} from out-of-control to in-control, the control chart leads to the conclusion, that, with respect to CP^{R^2} and CP^{MBox} , the system remains in a normal state during observation. Taking the percentage of out-of-control points as a first quality index, one can compare the different classifications and CPs. Table 1 shows the outlier percentage for all five classifications and 8 CPs. Here, standard statistical values (first three CPs) result in moderate outlier percentages. For these CPs, average values are given for all 24 channels since the CPs are calculated for each sensor. Further, tracking the first modal frequency results in larger outlier percentages. Dividing the training data into more clusters to capture the dynamic behavior in even more detail might resolve this problem. AE, SSI- and VAR-residues show good results for the AP classifications with few outliers. The manual classifications results in a large number of false alarms. Classifications with more EOCs included tend to perform better. The two outlier percentages belonging to the control charts in Fig.5(b) are highlighted.

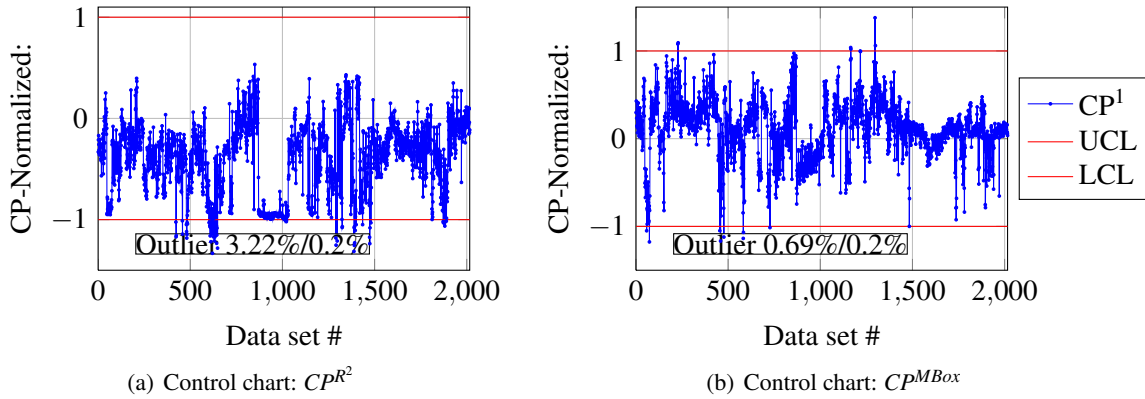


Figure 5 : Normalized control charts over a period of two weeks (2016 10 min sets) for two VAR-residues: CP^{R^2} (5(a)) and CP^{MBox} (5(b)). Upper- and lower control limit (UCL/LCL) are marked with red lines.

Table 1 : Percentage of false positive alarms for different CPs and classifications

Classification set-up	Manual	AP1	AP2	AP3	AP4
Used EOCs ²	[1,2]	[1,2]	[1-5]	[1-7,11]	[1-13]
No. of Clusters	4	13	7	8	11
Skewness (for each channel)	2.2	2.3	1.4	1.6	1.2
Kurtosis (for each channel)	2.3	2.9	1.9	1.8	1.5
Significant acceleration (for each channel)	6.3	3.5	1.5	2.1	1.8
2nd modal frequency	5.7	4.2	7.2	4.7	7.7
Accumulated Energy (90-100% energy level)	10.9	2.5	1.9	2.3	1.8
Nullspace based SSI Residue	3.7	1.9	1.1	0.8	0.5
VAR- R^2 Residue	77.4	5.7	3.2	2.0	1.1
VAR-MBox Residue	23.0	1.8	0.7	1.3	0.8

CONCLUSIONS

It is concluded, that every SHM approach necessitates, consists of, and can be categorized in three main steps: Condition parameter, machine learning, and hypothesis testing. This leads to a modular SHM-scheme, which was presented and applied to an offshore wind turbine using 10 min data sets recorded over a period of more than one year. Response data from accelerometers along with measured environmental and operational conditions, serve as input for the SHM-scheme. Machine learning, the calculation of condition parameters and hypothesis testing through the estimation of probabilistic models for those parameters lead to normalized control charts that can be easily evaluated and compared to provide observability. Giving the ability to include different machine learning algorithms and condition parameters, the scheme is generally applicable to structures in civil and mechanical engineering. Further, all applied combinations of machine learning and condition parameters result in false positive alarms from the control charts, which allow a good comparison. The investigated 5 MW offshore wind turbine remained in healthy condition throughout training and testing. Data classification through Affinity Propagation was used as machine learning technique and different condition parameters were implemented. The known healthy conditions are in agreement with the drawn control charts, where, with smaller and larger numbers of outliers, the control variable remains within the limits without suffering from strong shifts. Other control charts, e.g. with rational subgroups, can be introduced in future work as desired. Also, further EOC combinations and classification set-ups should be tested along with additional condition parameters.

REFERENCES

- [1] A. Rytter. *Vibration based inspection of civil engineering structures*. PhD thesis, Aalborg University, Denmark, 1993.
- [2] Moritz W. Häckell and Raimund Rolfes. Monitoring a 5MW offshore wind energy converter—Condition parameters and triangulation based extraction of modal parameters. *Mechanical Systems and Signal Processing*, 40(1):322–343, October 2013.
- [3] Moritz W. Häckell and Raimund Rolfes. Long-term monitoring of modal parameters for SHM at a 5 MW offshore wind turbine. In *Proceedings of the 9th International Workshop on Structural Health Monitoring*, pages 1310–1317, Stanford, CA, USA, 2013. Chang, F.-K. (Ed.), DEStech Publications Inc.
- [4] Luciano da Fontoura Da Costa and Roberto Marcondes Cesar. *Shape analysis and classification: theory and practice*. Image processing series. CRC Press, Boca Raton, FL, 2001.
- [5] Haruo Takizawa and Paul C. Jennings. Collapse of a model for ductile reinforced concrete frames under extreme earthquake motions. *Earthquake Engineering & Structural Dynamics*, 8(2):117–144, 1980.
- [6] Claus-Peter Fritzen and Peter Kraemer. Vibration based damage detection for structures of offshore wind energy plants. In *Proceedings of the 8th International Workshop on Structural Health Monitoring*, pages 1656–1663, Stanford, CA, USA, 2011. Chang, F.-K. (Ed.), DEStech Publications Inc.
- [7] H. Sohn, K. Worden, and C. R. Farrar. Statistical damage classification under changing environmental and operational conditions. *Journal of Intelligent Material Systems and Structures*, 13(9):561–574, September 2002.
- [8] Hoon Sohn, Charles R. Farrar, Norman F. Hunter, and Keith Worden. Structural health monitoring using statistical pattern recognition techniques. *Journal of Dynamic Systems, Measurement, and Control*, 123(4):706, 2001.
- [9] A. Deraemaeker, E. Reynders, G. De Roeck, and J. Kullaa. Vibration-based structural health monitoring using output-only measurements under changing environment. *Mechanical Systems and Signal Processing*, 22(1):34–56, January 2008.
- [10] K. Worden, H. Sohn, and C.R. Farrar. Novelty detection in a changing environment: Regression and interpolation approaches. *Journal of Sound and Vibration*, 258(4):741–761, December 2002.
- [11] B. J. Frey and D. Dueck. Clustering by passing messages between data points. *Science*, 315(5814):972–976, February 2007.
- [12] Delbert Dueck. *Affinity Propagation: Clustering Data by Passing Messages*. PhD thesis, University of Toronto, Graduate Department of Electrical & Computer Engineering, 2009.
- [13] Hoon Sohn, Mark Dzwonczyk, Erik G. Straser, Anne S. Kiremidjian, Kincho H. Law, and Teresa Meng. An experimental study of temperature effect on modal parameters of the alamosa canyon bridge. In *of the Alamosa Canyon Bridge.* *Earthquake Eng. and Structural Dynamics*, page 879–897. John Wiley & Sons, 1999.
- [14] Chengyin Liu and John T. DeWolf. Effect of temperature on modal variability of a curved concrete bridge under ambient loads. *Journal of Structural Engineering*, 133(12):1742–1751, December 2007.
- [15] Yilan Zhang, Moritz W. Häckell, Jerome Peter Lynch, and Raimund Rolfes. Automated modal parameter extraction and statistical analysis of the new carquinez bridge response to ambient excitations. In *Proceedings of the 32nd International Modal Analysis Conference (IMAC)*, Orlando, Florida, USA, 2014.
- [16] Spilios D. Fassois and John S. Sakellariou. Statistical time series methods for SHM. In Christian Boller, Fu-Kuo Chang, and Yozo Fujino, editors, *Encyclopedia of Structural Health Monitoring*. John Wiley & Sons, Ltd, Chichester, UK, September 2009.
- [17] Cecilia Surace and Keith Worden. Novelty detection in a changing environment: A negative selection approach. *Mechanical Systems and Signal Processing*, 24(4):1114–1128, May 2010.
- [18] Michael Döhler, Laurent Mevel, and Falk Hille. Subspace-based damage detection under changes in the ambient excitation statistics. *Mechanical Systems and Signal Processing*, 45(1):207–224, March 2014.
- [19] John Neter, William Wasserman, Michael H Kutner, et al. *Applied linear statistical models*, volume 4. Irwin Chicago, 1996.
- [20] Douglas C Montgomery. *Introduction to statistical quality control*. Wiley, Hoboken, 5 edition, 2005.
- [21] Jyrki Kullaa. Distinguishing between sensor fault, structural damage, and environmental or operational effects in structural health monitoring. *Mechanical Systems and Signal Processing*, 25(8):2976–2989, November 2011.